ORNL/TM--9885

DE86 004640

ORNL/TM-9885
Distribution Category UC-20d

Engineering Physics and Mathematics Division

# Monte Carlo and Discrete Ordinates Calculations for 14-MeV Neutrons Streaming Through a Stainless Steel Duct: Comparisons with Experiment II*

R. T. Santoro, J. M. Barnes,+ R. G. Alsmiller, Jr., and J. D. Drischler

*Submitted for Journal publication
+Computing & Telecommunications



Date of Issue: December 1985

Research sponsored by
Office of Fusion Energy
U.S. Department of Energy

Prepared by the
Oak Ridge National Laboratory
Oak Ridge, Tennessee 37831
operated by
Martin Marietta Energy Systems, Inc.
for the
U.S. DEPARTMENT OF ENERGY
under Contract No. DE-AC05-840R21400

## TABLE OF CONTENTS

## ABSTRACT

Measured and calculated neutron energy spectra from 14-MeV neutrons streaming through stainless steel ducts having length-to-diameter ratios of 14.8 and 38.2 are compared in this paper. The measured data were obtained using an NE-213 liquid scintillator and the calculated data were obtained using the Monte Carlo code MCNP and the discrete ordinates code DOT 4.3. For both duct geometries, the spectra calculated using the MCNP code are in reasonable agreement with the measured data ranging from a few percent to a factor of two, depending on the detector location and duct. The spectra calculated using the DOT code are in fair agreement (30%) for cases where the detector is on the duct axis, but are in poor agreement, up to an order of magnitude, when the detector is off axis.

## I. Introduction

Measured and calculated neutron energy spectra from 14-MeV neutrons streaming through cylindrical stainless steel Type 304 ducts having length-to-diameter (L/D) ratios of 14.8 and 38.2 are compared in this paper. In a previous paper, Ref. 1, similar data were compared for neutrons streaming through a stainless steel duct having an L/D ratio of 4.62. The measured data reported here, along with those given in Ref. 1, were obtained to validate the radiation transport codes and nuclear data that are being used in fusion reactor design calculations. As in previous papers,[1,2] the experimental configuration is representative in material composition and L/D ratio to the cylindrical ducts that will be found in fusion reactors.

With a few minor exceptions, the experimental procedures and methods of calculation used in this study are the same as those described in Ref. 1. The measured spectra were obtained using an NE-213 liquid scintillator detector with pulse-shape discrimination to separate neutron and gamma-ray events. The calculated data were obtained using the Monte Carlo code MCNP[3] and the discrete ordinates code DOT-4.3.[4] Details of the experimental configuration and the methods used in the measurements and calculations are summarized in Section II. The measured and calculated neutron energy spectra are compared in Section III.

## II. Experimental and Calculational Methods

### A. Experimental Details

The experiments were performed using the 14-MeV generator and experimental facility described in Ref. 1. The duct configurations used here were constructed from commercially available stainless steel Type-304 pipes imbedded in 1.45-m-thick concrete blocks. In the case of the L/D = 14.8 configuration, a pipe having an inside diameter of 0.098 m and a wall thickness of 0.0016 m was used. For the L/D = 38.2 configuration, the inside diameter of the pipe was 0.038 m with a wall thickness of 0.0035 m. The duct–concrete block assembly was mounted in a concrete support-shield structure so that the duct was coaxial with the deuteron-target axis with the front end of the duct located 0.82 m from the neutron source. The source neutrons were produced from the reactions of 250-keV deuterons incident on a 4-mg/cm$^2$-thick titanium-tritide target via the D-T fusion reaction.

The neutron spectra were measured with an NE-213 liquid scintillator. The detector, neutron bias levels, response functions, and the normalization procedures are the same as those described in Ref. 1.

### B. Calculational Details

The neutron energy spectra were calculated using both Monte Carlo and discrete ordinates methods. The calculations were performed using the two-dimensional model of the experimental assembly shown in Fig. 1. The experiment support-shield assembly, the iron can surrounding the target, and the SS-304 ducts were modelled in r-z geometry with cylindrical symmetry about the duct axis. A two-dimensional calculational model was adopted since the experimental configuration is essentially symmetric about the beam axis.

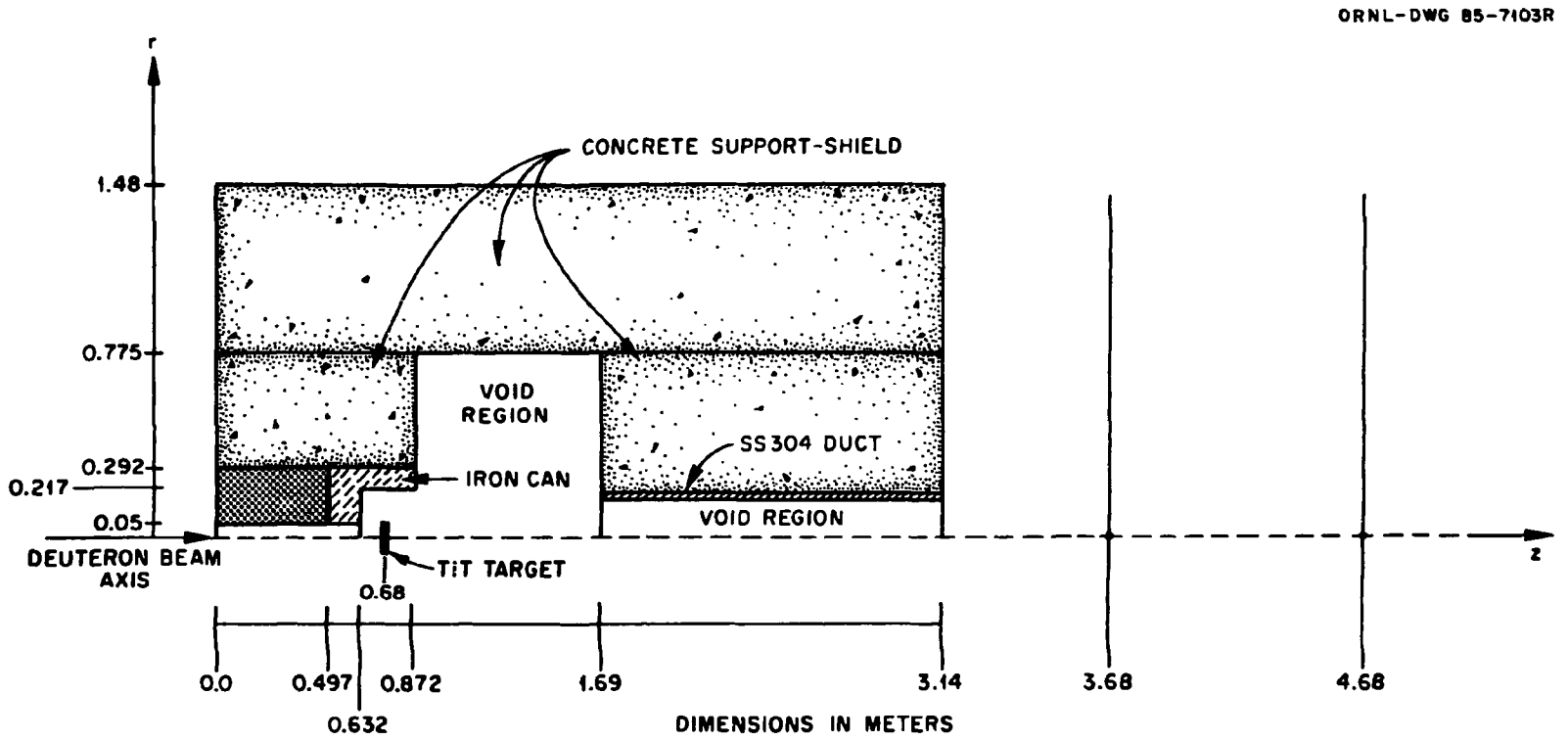


**Fig. 1. Two-dimensional calculational model of the experiment geometry.**

The experiment assembly rests on a concrete block stand which is lower in mass than the duct–concrete block assembly and the concrete surrounding this assembly, so omitting the stand from the calculational model does not significantly impact the calculated results. The spectra calculated using this geometry were compared with spectra calculated using a three-dimensional model as well as with measured data. All were in agreement, indicating that the two-dimensional geometry shown in Fig.1 is appropriate for these calculations.[1]

The Monte Carlo calculations were performed in a different manner than those reported in Refs. 1 and 2. In the former studies. the calculations of the energy spectra were carried out in two steps. The neutron fluxes per unit energy were calculated separately for neutrons emitted from the source in the forward and backward directions and the results were combined to yield the total flux. The options provided in the MCNP code for sampling neutrons from the source in energy and angle were used.

For the calculations performed here, a subroutine was written for MCNP to sample from the neutron source so that the neutron flux could be estimated in a single calculation. Since the duct diameters considered in this study are much smaller than the diameter of the duct considered in the previous work, the neutron source was biased to allow for a larger sample of particles to be emitted in the direction of the duct mouth. Neutrons emitted in the direction of the duct mouth were sampled with a probability of 0.87. The remaining neutrons were assumed to be emitted from the target uniformly in angle with a probability of 1.0−0.87. The neutrons emitted in the forward direction were assigned weights given by

$$W_{10^\circ} = W' (1-\cos\theta)/2p , \qquad (1)$$

where $W'$ is the unbiased source particle weight ($W' = 1$), $\theta$ is the polar angle of emission of the neutron from the target, and p is the probability for neutron emission in the forward direction. Neutrons emitted at all other angles were assigned weights according to

$$W_{>10^\circ} = W' (1-\cos\theta)/(2(1-p)) . \qquad (2)$$

For a source population of N neutrons, the unit particle weight in the combined calculation must also be unity, so that $W_{10^\circ} + W_{>10^\circ} = 1$. Thus,

$$\frac{pNW_{10^\circ} + (1-p)NW_{>10^\circ}}{N} = 1 , \qquad (3)$$

and unit weight is preserved.

The neutrons produced in the D-T reaction have an energy-angle dependence that must be accounted for in the calculations to assure that the measured and calculated energy spectra are compared to the same neutron source. The probabilities for the emission of the source neutrons in the energy interval $\Delta E$ and angular interval $\Delta\theta$ for the reactions of 250-keV deuterons incident on a 4-mg/cm-thick titanium tritide target are given in Table 1.[5]

**Table 1. Angle–Energy Dependence of Neutrons Emitted from the T(d,n)He Reaction (Deuteron energy = 250 keV)**

| Energy Interval (MeV) | Angular Interval (deg) | |
|---|---|---|
| | **0-40** | **40-180** |
| 14.92-15.68 | 0.0234 | - |
| 14.55-14.92 | 0.0827 | 0.0837 |
| 14.19-14.55 | 0.0148 | 0.2346 |
| 13.80-14.19 | - | 0.2581 |
| 13.50-13.80 | - | 0.2232 |
| 12.84-13.50 | - | 0.0776 |
| **Total** | **0.1209** | **0.8791** |

The Monte Carlo calculations were carried out using the MCNP code, Version 3, that is maintained at the National Magnetic Fusion Energy Computer Center (NMFECC) at Lawrence Livermore Laboratory. The neutron fluences were calculated using point estimators. Russian roulette and particle splitting were used to reduce the variance in the estimated results. The particle splitting parameters were obtained with the importance generator in MCNP. ENDF/B-V transport cross sections from the RMCCS 12 and RMCCS 13 data files were used. The compositions of the materials used in the calculations are given in Table 2.

The discrete ordinates calculations of the neutron energy were carried out in the same manner as those reported in Ref. 1. As in the previous work, the discrete ordinates calculations were performed using a $P_3$ Legendre expansion to describe the angular dependence of the scattering cross sections and an $S_{12}$ angular quadrature set. A discrete ordinates method using $P_3$ $S_{12}$ approximations is recognized to be inappropriate for the analysis of radiation streaming through ducts of very small diameter, but the analysis is included here only for completeness. The inadequacy of $P_3$ $S_{12}$ data has been demonstrated in previous studies.[1,2] As before, no attempt was made to incorporate a biased quadrature set since, in general, the selection of biased data are problem dependent and the results obtained using such data may not be appropriate in all cases. The selection of a higher order angular quadrature set was not considered since severe penalties in the code running time would have been incurred with little assurance of significant improvement in the results.

A 53-neutron, 22-gamma-ray energy group cross–section library obtained from the VITAMIN E library[6] was used in the calculations.

## III. Discussion of Results

The neutron energy spectra were measured and calculated for detectors located on and off the duct axis. The detector was located at a source-to-detector location (measured along the duct axis) of 3.0 or 4.0 m and, depending on the duct configuration, at distances perpendicular to the duct axis of 0.0, 0.1, or 0.2 m. The neutron energy spectra were compared for neutrons with energies above 850 keV.

In all of the figures shown below, the solid curves show the measured data and the open circles and the solid squares show the Monte Carlo and discrete ordinates results, respectively. Where two solid curves appear, they indicate a 68% confidence interval in the measured spectrum. The error bars on the Monte Carlo results indicate plus and minus one standard deviation. The Monte Carlo calculations were run using a neutron source population sufficient to obtain a standard deviation of $\pm 5\%$ in the neutron flux per unit energy above 10-MeV for the detectors on the duct axis.

The calculated data have been smoothed by convoluting the neutron flux per unit energy with an energy-dependent Gaussian response function having a width determined from the energy resolution of the NE-213 detector.[1,2] The neutron response matrix used in the unfolding of the energy spectra from the measured pulse–height data was obtained using the Oak Ridge Linear Accelerator.

**Table 2. Composition of Materials**

| | Composition (atom/barn·cm) | | | |
|---|---|---|---|---|
| **Element** | **Concrete** | **Air** | **Iron** | **SS-304** |
| H | 7.86-3 | | | |
| N | | 3.64-5 | | |
| O | 4.39-4 | 9.74-6 | | |
| Na | 1.05-3 | | | |
| Mg | 1.40-5 | | | |
| Al | 2.39-3 | | | |
| Si | 1.58-2 | | | |
| K | 6.90-4 | | | |
| Ca | 2.92-3 | | | |
| Cr | | | | 1.77-2 |
| Mn | | | | 1.77-3 |
| Fe | 3.10-4 | | 8.48-2 | 6.02-2 |
| Ni | | | | 7.83-3 |

The measured and calculated spectra are normalized to a source strength of one D-T neutron. The normalization for the measured data was determined using the associated particle counting method with a silicon surface barrier detector to count the neutrons from the D-T reaction. The neutron yield from the target is known within ±3%.

During the course of these measurements, a concrete shield that was normally used to cover the top of the experiment assembly was not in place. Consequently, the background radiation in the room was enhanced by radiation "spilling" out of the top of the experiment assembly. This problem was discovered as a result of the analysis. Since time constraints did not permit repetition of the experiment, and since the experimental assembly had been reconfigured with a solid concrete block in place of the duct geometry, a series of measurements were made to assess the magnitude of the background radiation with the concrete top present and absent. The data acquired from these measurements provided an estimate of the background which could be used to correct the measured spectra obtained during the duct streaming experiments. An uncorrected spectrum is shown in Fig. 2. The point to note from this figure is the large difference between the measured and calculated data in the energy range below 3.0 MeV. In the figures shown below, the differences between the calculated and measured spectra in this energy range have been reduced as the result of the background correction.

### A. L/D = 14.8 Duct Configuration

The radiation streaming through the L/D duct was assessed by comparing the measured and calculated differential neutron energy spectra at a source-to-detector distance measured along the duct axis of 3.0 m and at distances perpendicular to the duct axis of 0.0, 0.1, and 0.2 m. The measured and calculated neutron spectra are compared in Figs. 3–5.

For the case where the detector is on the duct axis, Fig. 3, the spectrum calculated using the MCNP code is in very good agreement with the measured spectrum at all energies. The spectrum calculated with the DOT code is lower than the measured spectrum at neutron energies above 13 MeV but is in good agreement with the measured data at energies below 13 MeV. When the detector is on the duct axis, the principal contribution to the neutron spectrum is from the uncollided neutrons from the source. A small fraction of the neutrons scatter to the detector from the SS-304 duct liner and from the concrete immediately surrounding the duct. The Monte Carlo results suggest that 10% of the neutron flux above 13 MeV is due to these scattered neutrons. The $S_{12}$ angular quadrature used in the DOT calculation is too coarse to properly account for these neutrons, so the neutron flux above 13 MeV is underestimated.

For the cases where the detector is off the duct axis, r = 0.1 and 0.2 m, shown in Figs. 4 and 5, respectively, the agreement between the measured and calculated data is less favorable. The spectra calculated with MCNP reproduce the measurement in shape but not in magnitude. The calculated flux above 13 MeV and below 6 MeV is low compared to the measurement. The spectra obtained with the DOT code are in poor agreement with both the measured and the MCNP spectra at neutron energies above 12 MeV but are in good agreement with the MCNP data below 6 MeV, albeit both the Monte Carlo and discrete ordinates spectra are lower than the measured data.

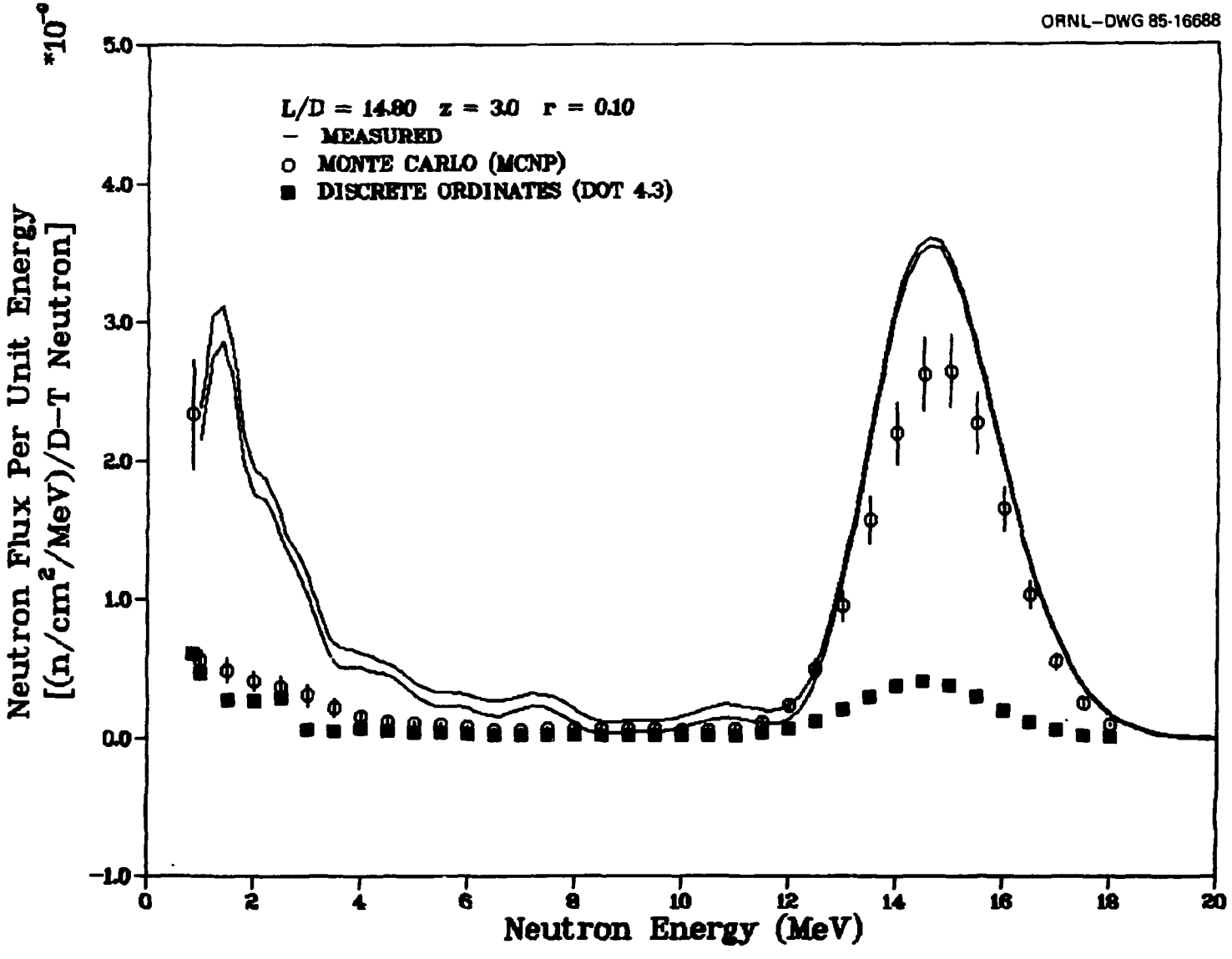


**Fig. 2. Neutron flux per unit energy versus neutron energy for the detector at z = 3.0 m and r = 0.1 m.** L/D = 14.8 duct configuration. Note the large difference between the calculated an experimental spectra at neutron energies below 3.0 MeV. This difference arises from the large room background.

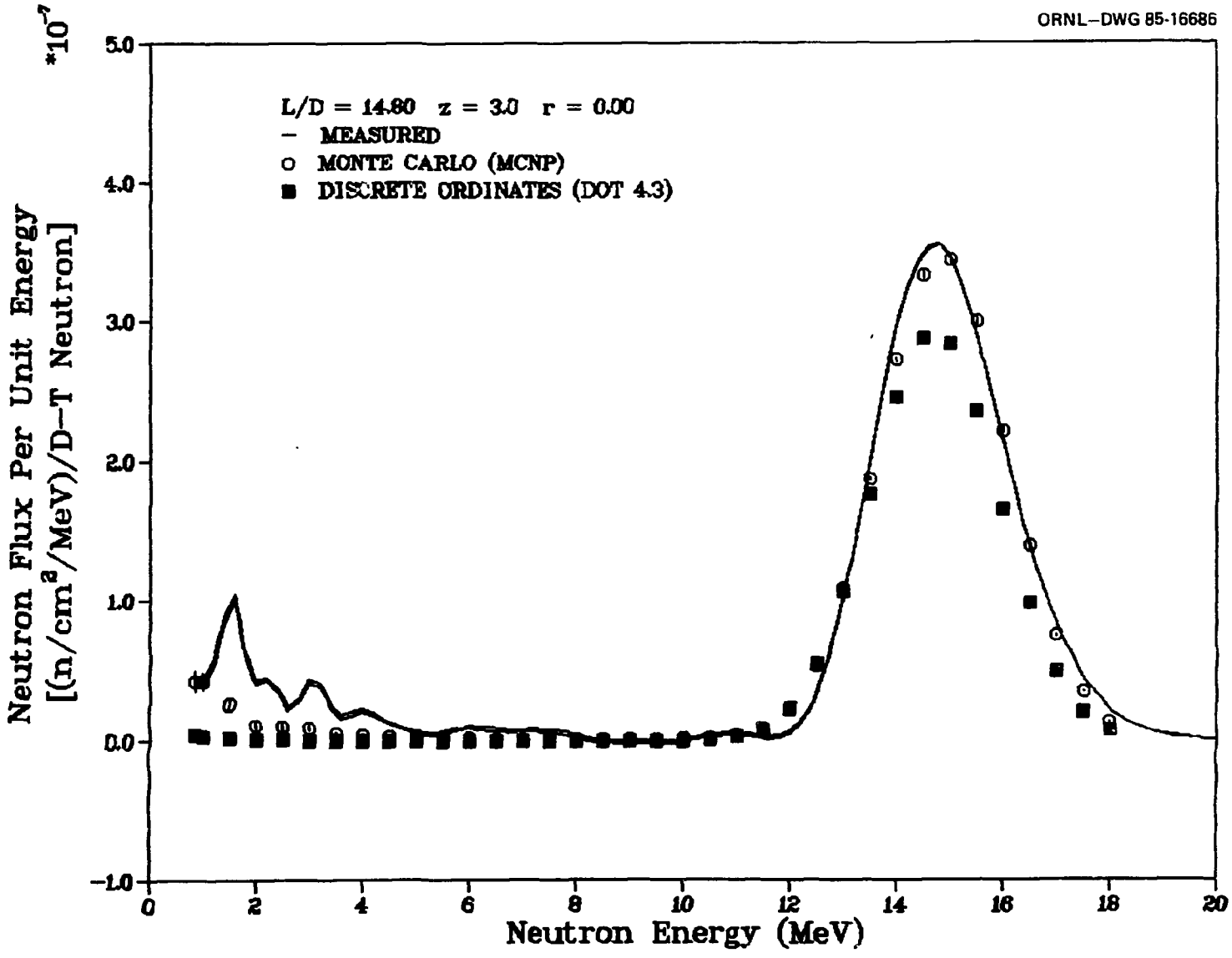


**Fig. 3. Neutron flux per unit energy versus neutron energy for the detector at z = 3.0 m and r = 0.0 m.** L/D = 14.8 duct configuration.

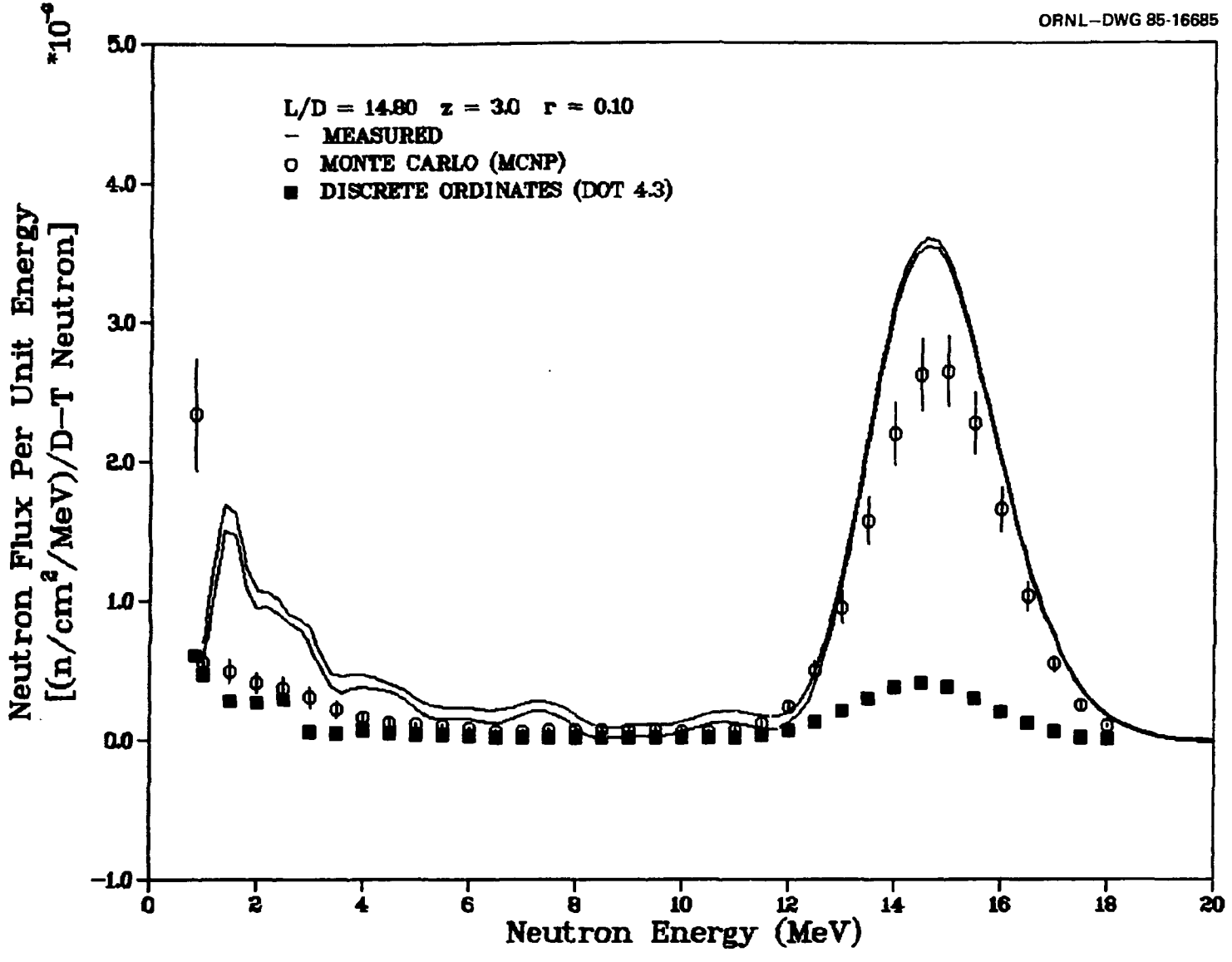


**Fig. 4. Neutron flux per unit energy versus neutron energy for the detector at z = 3.0 m and r = 0.1 m.** L/D = 14.8 duct configuration.

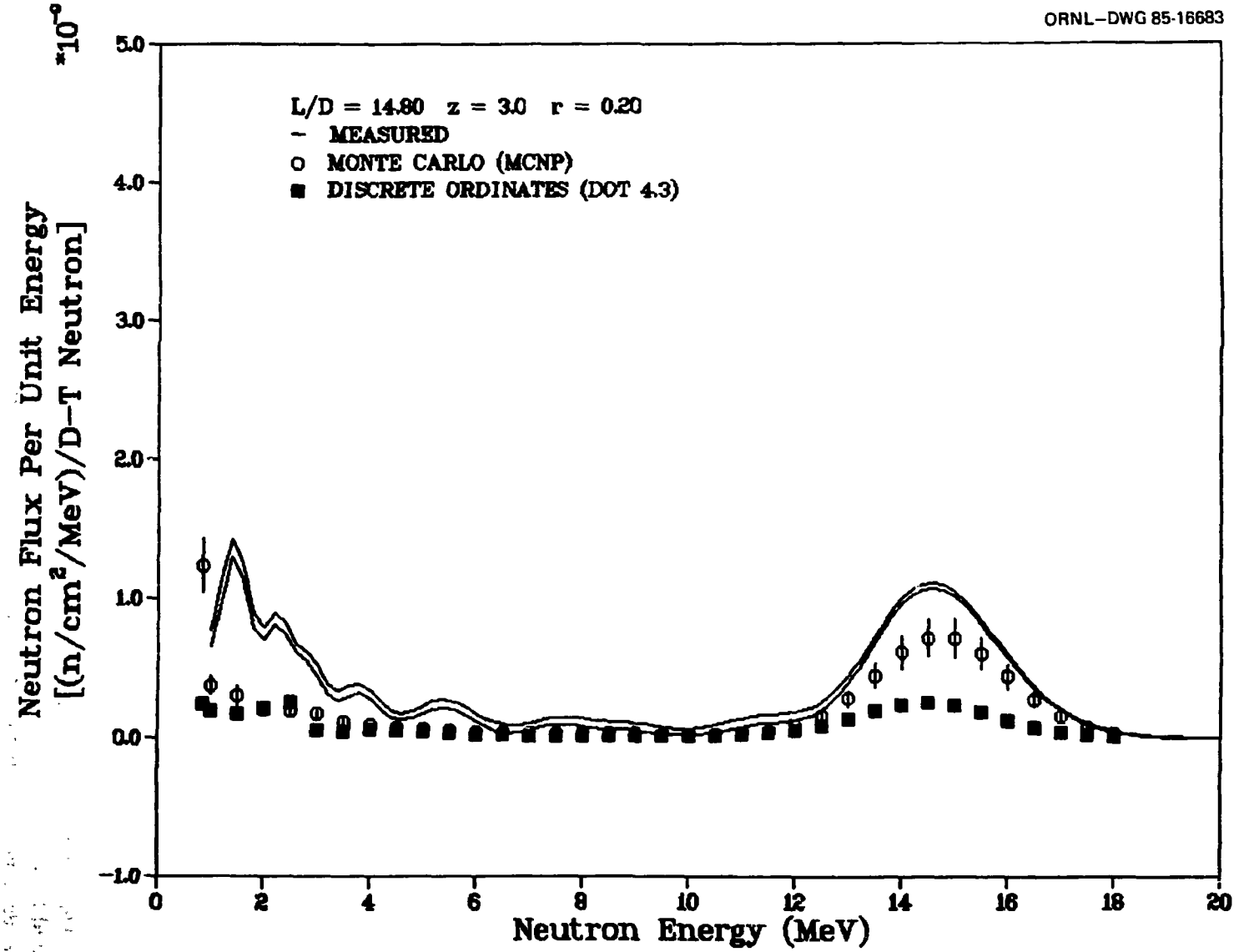


**Fig. 5. Neutron flux per unit energy versus neutron energy for the detector at z = 3.0 m and r = 0.2 m. L/D = 14.8 duct configuration.**

### B. L/D = 38.2 Duct Configuration

The measured and calculated differential neutron energy spectra for the L/D = 38.2 duct configuration are compared in Figs. 6 and 7. The spectra are compared at a source-to-detector distance of 4.0 m and at distances perpendicular to the duct axis of 0.0 and 0.1 m. For the case where the detector is on the axis, the spectrum calculated using the MCNP code is in good agreement with the measured spectrum at all energies. The spectrum calculated using the DOT code lies below the measured spectrum and that calculated by the MCNP code at neutron energies above 13 MeV but is in good agreement with the measured and MCNP spectra at lower energies. For the off-axis detector location, the agreement between the measured spectrum and the spectra calculated using both transport methods is poor at neutron energies above 13 MeV. The MCNP data reproduce the spectrum in shape but the magnitudes are low by about a factor of two. The spectrum calculated using the DOT code is in very poor agreement with both the measured and the MCNP data and it exhibits the same behavior as observed for the off-axis comparisons given for the L/D = 14.8 duct configuration.

### C. Comparisons of Integral Data

The measured and calculated integral neutron spectra for the L/D duct configurations are compared in Tables 3 and 4, respectively. These data were obtained by integrating the differential spectra over energy. The integrated spectra are also compared in the tables in terms of the calculated to experimental (C/E) ratios of the spectra above 10 and 1 MeV. The integral of the measured spectra are given in the table.

For the L/D = 14.8 duct geometry, the data obtained with the MCNP code for the case where the detector is on axis is in good agreement (10%) with the measured spectrum at all neutron energies. The spectrum calculated with the DOT code, on the other hand, underpredicts the measurement by 20% at neutron energies above 10 MeV and by 30% at neutron energies above 1 MeV. For the off-axis detectors, the agreement among the integral data obtained using both calculational methods is poor. The Monte Carlo data differ from the measurement by as much as a factor of two, while the discrete ordinates data differ by as much as an order of magnitude.

For the L/D = 38.2 duct, the Monte Carlo calculation reproduces the measurement within 10% at all neutron energies for the on-axis detector and within a factor of two for the off-axis case. The spectra calculated using the DOT code differ with the measured data from a factor of two to an order of magnitude, depending on detector location and energy.

## IV. Observations and Conclusions

The differences among the measured and calculated spectra shown above may be attributed to several factors. In the case of the MCNP spectra, some of the difference between the data may be attributed to the composition of the concrete and, in particular the amount of bound water in the concrete. It is difficult to obtain an accurate estimate of the amount of water contained in concrete so the composition used in the calculations can be uncertain, thereby leading to the observed differences in the results. Also, in the case of this study, the Monte Carlo code must simultaneously resolve a deep penetration and streaming problem both of which are formidable analysis problems.

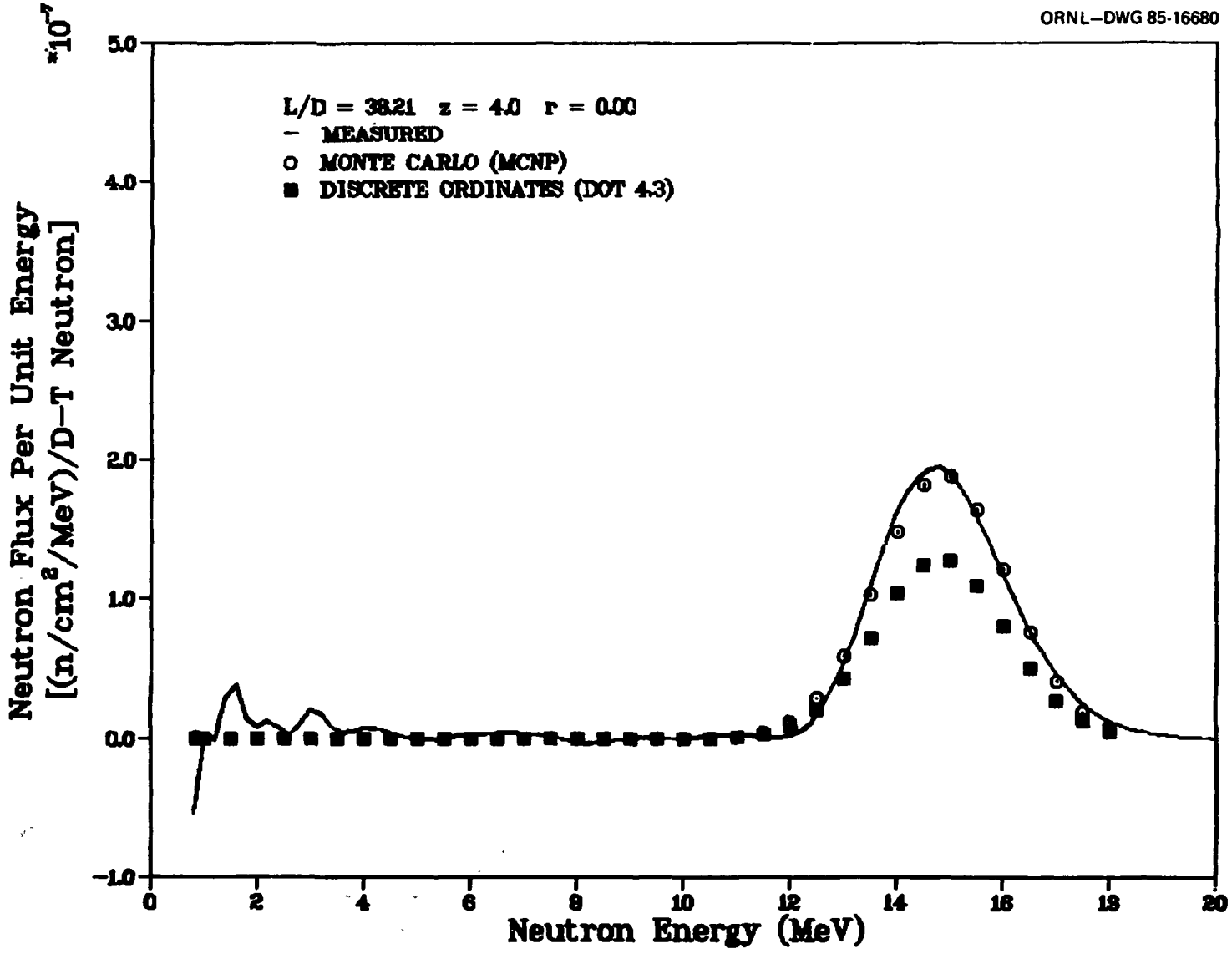


**Fig. 6. Neutron flux per unit energy versus neutron energy for the detector at z = 4.0 m and r = 0.0 m.** L/D = 38.2 duct configuration.

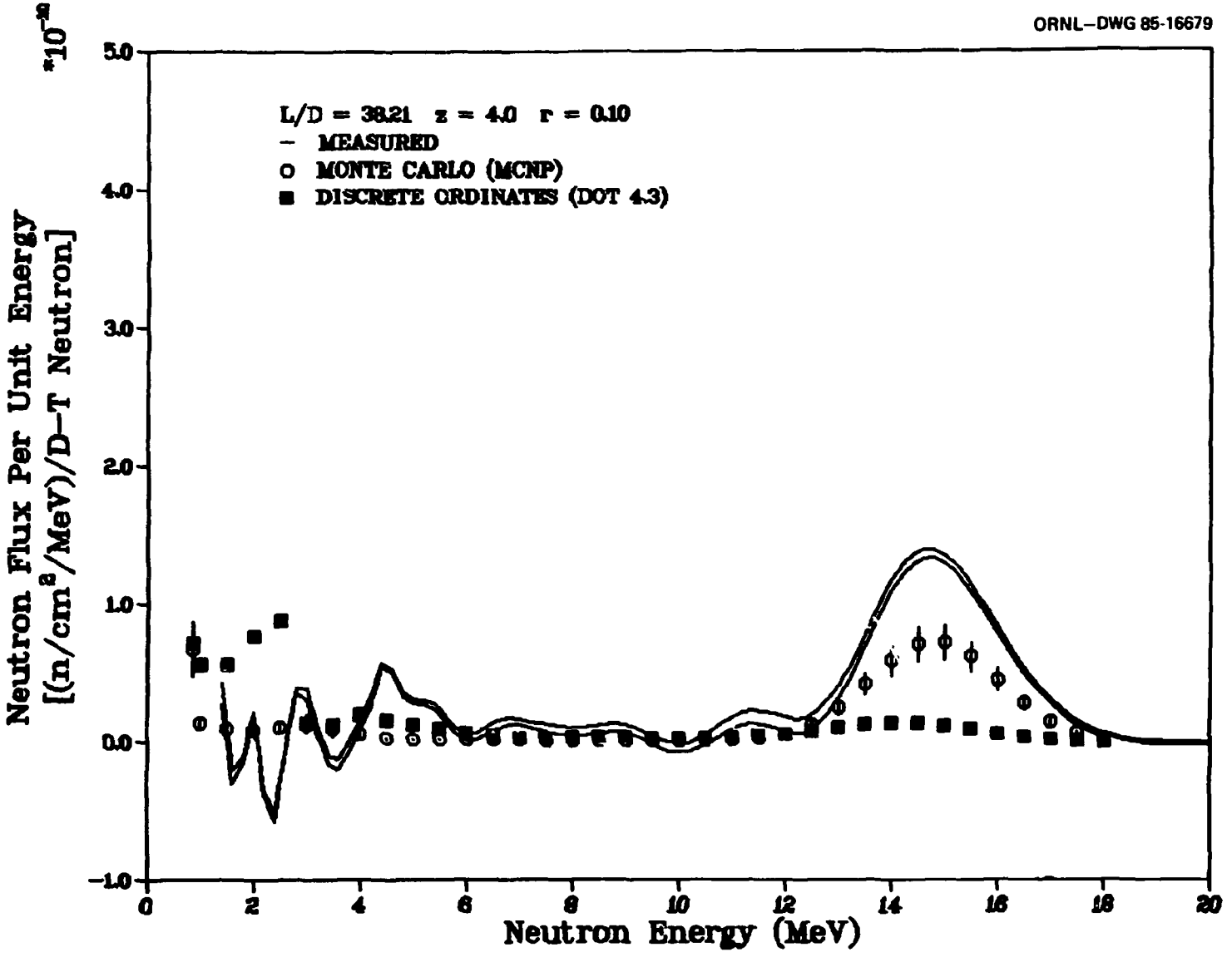


**Fig. 7. Neutron flux per unit energy versus neutron energy for the detector at z = 4.0 m and r = 0.1 m. L/D = 38.2 duct configuration.**

**Table 3. Comparison of Measured and Calculated Integral Neutron Spectra (L/D = 14.8 Duct Configuration)**

| Detector Location (m) | | Neutron Flux Above Energy E [(n/cm$^2$)/DT Neutron] | | | | | |
|---|---|---|---|---|---|---|---|
| z | r | 10 MeV[a] | C/E(MC)[b] | C/E(Sn)[c] | 1 MeV[a] | C/E(MC) | C/E(Sn) |
| 3 | 0.0 | 1.08-6[d] | 0.985 | 0.819 | 1.25-6 | 0.902 | 0.712 |
| 3 | 0.1 | 1.10-8 | 0.769 | 0.123 | 1.48-8 | 0.685 | 0.151 |
| 3 | 0.2 | 3.52-9 | 0.659 | 0.235 | 6.38-9 | 0.508 | 0.223 |

[a]Measured integral neutron flux above the energy indicated.
[b]Monte Carlo calculation to experimental neutron flux ratio.
[c]Discrete ordinates calculation to experimental neutron flux ratio.
[d]Read as $1.08 \times 10^{-6}$.

**Table 4. Comparison of Measured and Calculated Integral Neutron Spectra (L/D = 38.2 Duct Configuration)**

| Detector Location (m) | | Neutron Flux Above Energy E [(n/cm$^2$)/DT Neutron] | | | | | |
|---|---|---|---|---|---|---|---|
| z | r | 10 MeV[a] | C/E(MC)[b] | C/E(Sn)[c] | 1 MeV[a] | C/E(MC) | C/E(Sn) |
| 4 | 0.0 | 5.92-7[d] | 0.980 | 0.670 | 6.37-7 | 0.911 | 0.623 |
| 4 | 0.1 | 4.2-10 | 0.539 | 0.139 | 4.1-10 | 0.655 | 0.618 |

[a]Measured integral neutron flux above the energy indicated.
[b]Monte Carlo calculation to experimental neutron flux ratio.
[c]Discrete ordinates calculation to experimental neutron flux ratio.
[d]Read as $5.92\times10^{-7}$.

The type of geometry studied here is a difficult one for a DOT calculation. Streaming is, in general, a difficult problem for the discrete ordinates method and, in the approach taken here, where a low order expansion of the scattering data and a low order symmetric quadrature are used, the results obtained are expected to be marginal.

An important point to note from these results, as well as from those in Ref.1, is the rapid drop in the neutron flux as the detector is moved into the shadow of the duct. The uncollided neutrons dominate the spectrum when the detector is on the axis. When the detector is moved off the axis, the flux drops by nearly two orders of magnitude.

## REFERENCES


1. R. T. Santoro, J. M. Barnes, R. G. Alsmiller,Jr., and J. D. Drischler, "Monte Carlo and Discrete Ordinates Calculations of 14-MeV Neutrons Streaming Through a Stainless Steel Duct: Comparison with Experiment I," ORNL/TM-9541, Oak Ridge National Laboratory (1985).

2. R. T. Santoro, J. M.Barnes, K. G. Alsmiller,Jr., and P. D. Soran, *Nucl. Sci. Eng.* **84**, 260-270 (1983).

3. "MCNP - A General Purpose Monte Carlo Code for Neutron and Photon Transport," LA-7396-M (Rev.) Version 2B, Los Alamos National Laboratory (1981).

4. W. A. Rhoades and R. L. Childs, "An Updated Version of the DOT IV One- and Two-Dimensional Neutron/Photon Transport Code," ORNL-5851, Oak Ridge National Laboratory (1982).

5. R. T. Santoro, J. M. Barnes, J. D. Drischler, and R. G. Alsmiller,Jr., "Multigroup Energy-Angle Distributions for Neutron from the $T(d,n)^4He$ Reaction (E = 100-400 keV), ORNL/TM-9251, Oak Ridge National Laboratory (1984).

6. C. R. Weisbin, R. W. Roussin, J. J. Wagschal, J. E. White, and R. Q. Wright, "VITAMIN-E: An ENDF/B-V Multigroup Cross-Section Library for LMFBR Core and Shield, LWR Shield, Dosimetry, and Fusion Blanket Technology," ORNL-5505, Oak Ridge National Laboratory (1979).

**ORNL/TM-9885**
**Distribution Category UC-20d**

*INTERNAL DISTRIBUTION*

1–3. L. S. Abbott
4. F. S. Alsmiller
5–9. R. G. Alsmiller, Jr.
10–14. J. M. Barnes
15. L. A. Berry
16. D. G. Cacuci
17–21. J. D. Drischler
22–31. EPD Reports Office
32. T. A. Gabriel
33. R. A. Lillie
34. J. L. Lucius
35. F. C. Maienschein
36. R. W. Peelle
37. R. W. Roussin
38. M. W. Rosenthal
39–40. RSIC
41–45. R. T. Santoro
46. T. E. Shannon
47. C. R. Weisbin
48. A. Zucker
49. P. W. Dickson, Jr. (Consultant)
50. G. H. Golub (Consultant)
51. D. Steiner (Consultant)
52–53. Central Research Library
54. Fusion Energy Division Library
55. Fusion Energy Division Reports Office
56. ORNL Y-12 Technical Library Document Reference Section
57–58. Laboratory Records
59. ORNL Patent Office
60. Laboratory Records - RC

*EXTERNAL DISTRIBUTION*

61. Office of Assistant Manager for Energy Research & Development, DOE-ORO, Oak Ridge, TN 37830.

62. S. E. Berk, Division of Development and Technology, Office of Fusion Energy, ER-532, U.S. Dept. of Energy, Washington, D.C. 20545.

63. J. D. Callen, Dept. of Nuclear Engineering, University of Wisconsin Madison, WI 53706.

64. R. W. Conn, Dept. of Chemical, Nuclear and Thermal Engineering, University of California, Los Angeles, CA 90024.

65. S. O. Dean, Director, Fusion Energy Development, Science Applications, Inc., 2 Professional Dr., Suite 249, Gaithersburg, MD 20760.

66. B. Engholm, General Atomic Co., P.O. Box 81608, San Diego, CA 92138.

67. H. K. Forsen, Bechtel Group, Inc., Research Engineering, P.O. Box 3964, San Francisco, CA 94105.

68. Y. Gohar, Argonne National Laboratory, 9700 S. Cass Avenue, Argonne, IL 60439

69. R. W. Gould, Dept. of Applied Physics, California Institute of Technology, Pasadena, CA 92024.

70. D. G. McAlees, Exxon Nuclear Co., Inc., 777 106th Ave., N.E., Bellevue, WA 98009.

71. Library, Princeton Plasma Physics Laboratory, Princeton University, P.O. Box 451, Princeton, NJ 08540.

72. P. Sager, General Atomic Co., P.O. Box 81608, San Diego, CA 92138.

73. W. M. Stacey, Jr., School of Nuclear Engineering, Georgia Institute of Technology, Atlanta, GA 30332.

*EXTERNAL - FOREIGN*

74. Bibliothek, Institut fur Plasmaphysik, D-8046, Garching bei Munchen, Federal Republic of Germany.

75. Bibliothek, Institut fur Plasmaphysik, KFA, Postfach 1913, D-5170, Julich 1, Federal Republic of Germany.

76. Bibliotheque, Service du Confinement des Plasmas, CEA, B.P. No. 6, 92, Fontenay aux Roses (Seine), France.

77. Documentation, S.I.G.N., D.P.PFC. CEN, P.O. 85, Centre de Tri, 38041 Cedex, Grenoble, France.

78. Institute of Physics, Academia Sinica, Peking, Peoples Republic of China.

79. Library, Centre de Recherches en Physique des Plasmas, 21 Avenue des Bains, 1007, Lausanne, Switzerland.

80. Library, Culham Laboratory, UKAEA, Abingdon, Oxon, OX14-3DB, England.

81. Library, FOM Institute voor Plasma-Fysica, Rijnhuizen, Jutphass, Netherlands.

82. Library, Institute for Plasma Physics, Nagoya University, Nagoya 464, Japan.

83. Library, International Centre for Theoretical Physics, Trieste, Italy.

84. Library, Laboratoria Gas Ionizzati, Frascati, Italy.

85. Library, Plasma Physics Laboratory, Kyoto University, Gokasho Uji, Kyoto, Japan.

86. Plasma Research Laboratory, Australian National University, P.O. Box 4, Canberra ACT.2000, Australia.

87. Dr. Yasushi Seki, Japan Atomic Energy Research Institute, Tokai-mura, Ibaraki-ken, Japan.

88. Thermonuclear Library, Japan Atomic Energy Research Institute, Tokai, Naka, Ibaraki, Japan.

89. R. Varma, Physical Research Laboratory, Navangpura, Ahmedabad, India.

90. Dr. Michinori Yamauchi, Nippon Atomic Industry Group Co., Ltd., NAIG Nuclear Research Laboratory, 4-1, Ukishima-cho, Kawasaki-ku, Kawasaki City, 210, Japan.

91-211. Given distribution as shown in TID-4500, Magnetic Fusion Energy (Distribution Category UC-20d: Fusion Systems).